

## REMOVAL OF RANDOM NOISE FROM CONVENTIONAL DIGITAL X-RAY IMAGES

Dr. Khalil I. Jassam, Researcher, the Institute of Islamic Medicine for Education and Research Panama City, FL. and a visiting professor, and Maureen Carr, Department of Surveying Engineering University of Maine Orono, ME. USA

Commission No: VII

### ABSTRACT:

Conventional X-ray imaging is the fastest, most common, and least expensive diagnostic imaging system available. Production of digital X-rays from pictorial radiographs is becoming a common practice to maximize information and reduce the number of rejected X-rays. Secondary radiation, film processing and handling, and digitization are the main sources of noise in digital X-ray images. The aim of this paper is to present the best procedure for noise suppression in digital X-ray images by applying conventional noise filtering techniques in the spatial and frequency domains. The resulting X-ray images are more visible, although fine details may be lost. In addition, filtering in the frequency domain appears to maintain image integrity better than that of the spatial domain.

Key Words: X-ray imaging, Image Processing, Medical Imaging, Noise removal

### INTRODUCTION

X-rays were discovered in 1895 by the German physicist Roentgen and were so named because their nature was unknown at the time. Unlike ordinary light, these rays are invisible, but they travel in straight lines and effect photographic film in the same way as light. On the other hand, they are much more penetrating than light and could easily pass through the human body, wood, and other "opaque" objects. We know today that X-rays are electromagnetic radiation of exactly the same nature as light but of very much shorter wavelength. The unit of measurement in the X-ray region is the angstrom ( $\text{\AA}$ ), equal to  $10^{-8}$  cm. X-rays, used in diffraction, have wavelengths lying approximately between the range of 0.5 - 2.5  $\text{\AA}$ , where the wavelength of visible light is on the order of 6000  $\text{\AA}$ . X-rays, therefore, occupy the region between gamma and ultraviolet rays in the electromagnetic spectrum.

The method employed to produce X-rays is essentially the same as that used at the time of its discovery. A beam of electrons, accelerated by high voltage to a velocity approaching the speed of light, is rapidly decelerated upon colliding with a heavy metal target. In the process of slowing down, X-ray photons are emitted; the emitted X-rays are then directed to the human body. The number of X-rays that interact with the patient depends upon the thickness and the composition of the various tissues. Diagnostic X-rays interact primarily by the photoelectric and Compton processes. Photoelectric interactions are the most important for image formation because of the strong dependence of the photoelectric effect on the atomic composition of the absorber and the absence of long-range secondary radiation. Compton interactions are generally detrimental in that the likelihood of their occurrence depends mainly on tissue density, and the scattered X-rays produced in Compton collisions have a high probability of escaping from the patient and crossing the image plane.

Because their directions are unrelated to the position of the focal spot, these scattered X-rays do not carry any useful information about the patient and serve only to reduce X-ray contrast. Unfortunately, the interaction of diagnostic X-rays with soft tissue is mainly by the Compton process, and specific stratagems must be employed to prevent "scatter" from reaching the imaging device. The X-ray image is determined by the intensity distribution in the X-ray beam as it emerges from the patient. The quality of the X-ray image, depends upon the focal-spot size, the incident X-ray spectrum, and the composition of the patient. Over many years the optimum parameters for a specific examination (e.g. X-ray tube potential, beam filtration, exposure time, infection of contrast media) have been empirically determined by a large number of practitioners.

At average diagnostic kilovoltage levels, about 5% or less of the primary radiation traverses completely through the patient's body, without interacting with any of the atoms in the patient, and strikes the film. In addition, about 15% of the primary radiation interacts with atoms resulting in the production of the secondary photons which make it out of the patient and strike the film. The remaining 80% of the primary beam is totally absorbed within the patient. The attenuation of an X-ray beam by the various tissues within the patient results in a variation of transmitted radiation. The pattern of transmitted radiation may be expressed in terms of variations in photon fluency, variations in energy fluency or variations in exposure.

X-ray images are formed in a manner similar to regular black and white pictures. Body parts which have higher resistance to X-ray penetration (bones) result in less light reaching the film and consequently brighter image on the X-ray transparency which is nothing more than a negative image. On the other hand, soft tissues have less resistance to X-rays, so more X-rays pass through them, resulting in more radiation reaching the film and producing darker tones. In most cases the bones are the brightest and gases are the darkest.

## SOURCES OF NOISE IN DIGITAL X-RAYS

There are three major sources of noise in conventional digital X-rays. The main source of noise is the so-called secondary radiation which is nothing more than reflected X-rays which reach the film from all directions. These unwanted X-rays tend to reduce the contrast quality of the image. Radiologists have solved the problem by developing a specially designed grid plate made of lead. The grid plate absorbs most of the scattered secondary X-ray and produces a radiograph within the acceptable level of noise (figure 1). This technique is the most popular method used in almost all traditional X-ray machines.

Another source of noise is film development and film handling, although the procedure is fully automated roughly 10 to 15% of the processed X-rays are poorly developed. Image with poor contrast quality whether over or under-exposed, is usually labeled as a rejected image. All rejected images are thrown away and the X-ray must be retaken. Rejected pictures make up 20% of the total number of X-rays taken per year (Jassam, 1992). The rejected pictures cost hospitals millions of dollars per year and expose the patient to unnecessary radiation.

With advancing computer technology and increasing public concern with both the radiation level and insurance costs, the need to transfer from pictorial to digital X-rays is growing rapidly. This transformation will introduce additional sources of noise both geometrically and radiometrically. The unblocked secondary radiation, poor film developing and handling, and the digitization process introduces noise into the digital X-ray. The noise to signal ratio is relatively high in the case of rejected images and within an acceptable limit otherwise. Image processing techniques proved to be effective in minimizing the number of rejected pictures (Jassam, 1992). To maximize the amount of information extracted from the X-ray images and to increase their visual quality, the noise has to be suppressed. Low-pass filters are often used in image processing to remove random noise from a digital image. Unfortunately, as noise is removed from an image, details in the image are also lost. The goal of removing noise in an image is therefore to strike a balance between noise and detail which is appropriate for the application at hand.

To determine this balance between noise and detail, the user applies a variety of low-pass filters, of various sizes, to the image and then compares the results. This comparison can either be quantitative; employing statistical analysis techniques, or qualitative; examining the physical appearance of the image. Both the statistical and physical results of applying low-pass filters to an X-ray image in the spatial and frequency domains, using Intergraph Corporation's Imager software (TIGRIS 1988), are addressed.

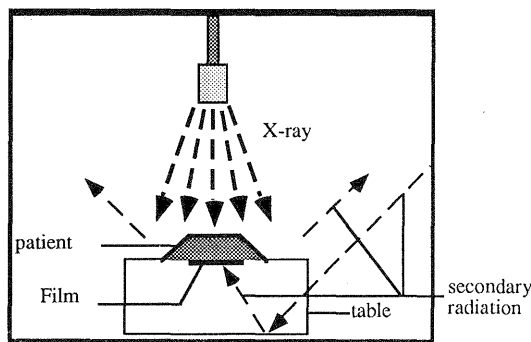


Figure 1. secondary radiation reach the film, are the main source of noise.

## TREATMENT OF NOISE IN DIGITAL X-RAY IMAGES

In the process of generating a digital image, many sources of error are encountered. These include errors in acquiring the data, errors in digitizing the data, and errors in transmitting the data. As a result of these errors, digital images often contain individual pixels which vary abruptly in intensity from their neighboring pixels and which do not reflect the scene they represent. These pixels are referred to as random noise (Richards, 1986). To remove noise, low-pass (smoothing) filters are applied to the image. It is important to note that noisy pixels are like edges and lines in that they stand out from their neighbors, and because of this similarity, removing noise in an image also results in removing, or at least blurring, edges and lines.

Filters can be applied in the spatial or the frequency domain. In the spatial domain, the values of the pixels in the resulting image depend directly upon their original values and the values of their original neighboring pixels. In the frequency domain, the resulting pixel values depend on the horizontal and vertical frequency components in the original image and not directly on individual pixel values (Richards, 1986). However, in both domains, low-pass filters serve to reduce the contrast amongst neighboring pixels, and since noisy pixels are pixels whose intensities vary abruptly from the intensities of neighboring pixels, applying low-pass filters reduces the amount of contrast and therefore the amount of noise in the image.

### Spatial domain

To filter an image in the spatial domain, a kernel is moved over the rows and the columns of the image and the value of the pixel located in the center of the kernel is replaced by the sum of the products of the kernel elements and the corresponding image pixel values (Richards, 1986). Mathematically, this can be expressed as follows:

$$g(x,y) = \sum_{m=1}^M \sum_{n=1}^N f(m,n)t(m,n) \dots\dots\dots 1$$

where :

- $g(x,y)$  is the image new brightness values,
- $M$  is number of rows in the kernel,
- $N$  is number of columns in the kernel,
- $f(m,n)$  is the pixel brightness value addressed according to the kernel position, and
- $t(m,n)$  is the kernel entry at that location.

The low-pass filter provides a way of removing noise by changing the pixel value of a noisy pixel to the average value of its surrounding pixels. However, not all pixels whose brightness values differ from surrounding pixels represent noise. Therefore, low-pass filtering results in less detail in addition to less noise. The size of the kernel determines the number of pixel values used to calculate the replacement pixel value. Therefore, larger kernels use more pixel values in the averaging process and this results in smoother images.

Other smoothing filters are the median, and the mode. The median filter functions similarly to the low-pass filter, however, the center pixel is replaced by the median value of the pixels covered by the filter. As a result the median filter is less likely to smooth edges. The mode filter also functions similarly to the low-pass filter, however, in this case the center pixel is replaced by the mode of the pixels covered by the filter.

A rejected underexposed X-ray with a high level of noise was selected (figure 2). The pre-processed histogram (figure 3) showed a low-radiance, low-contrast scene and a bi-mode image. In fact, the original image was so underexposed it was totally invisible without contrast enhancement. Since the image is a bi-mode, a piecewise equalizer was used to enhance it. The gray levels between 5 and 14 were stretched to between 50 and 255 while the rest of the image was not changed. Then the process was reversed and the gray levels between 15 and 30 were stretched to between 50 and 255. The two obtained enhanced images are shown in figures 4 and 5. By analyzing the two figures, it can be seen that the noise is the dominant feature in the image. The knee-cap and the tibia bone were almost totally lost.

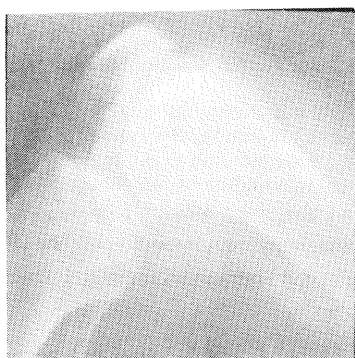


Figure 2. Histogram equalization of the original X-ray.

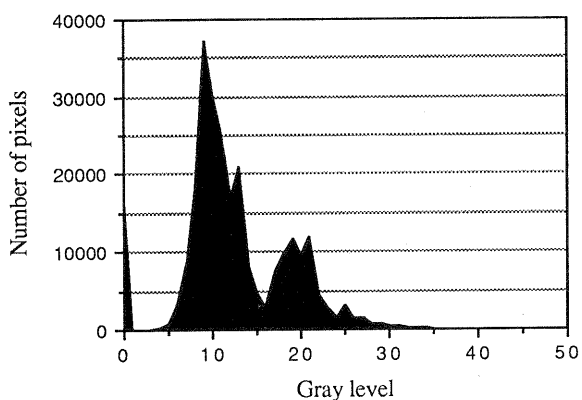


Figure 3. Histogram of the original image

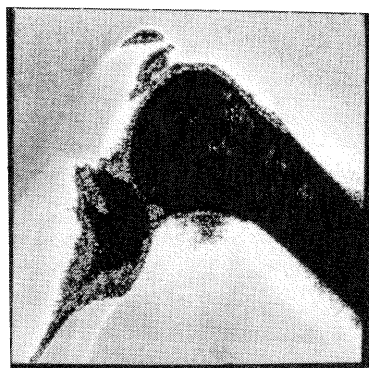


Figure 4. Piecewise equalized image for the gray values 5 to 14.

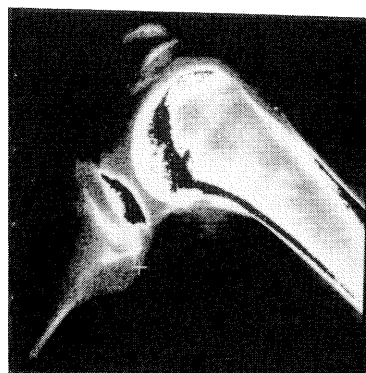


Figure 5. Piecewise equalized image for the gray values 15 to 30.

Low pass, median, and mode filters were applied to the image at different kernel sizes from  $3 \times 3$  to  $9 \times 9$ . At each kernel size the smoothed image was compared both visually and statistically with the original image and its histogram.

Figures 6, 7, 8, 9, 10, and 11 show the obtained histogram and the resultant image for  $3 \times 3$  and  $5 \times 5$  kernel size. It should be emphasized that all filters were applied to the original image prior to any enhancement because existing noise would be enhanced.



Figure 6. Spatial domain low pass filter  $5 \times 5$ .

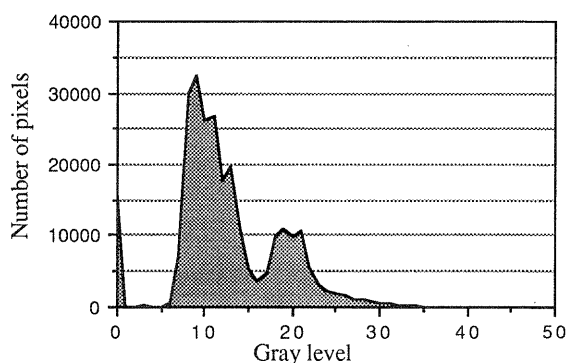


Figure 7. Histogram of low pass filter  $5 \times 5$  at 6.

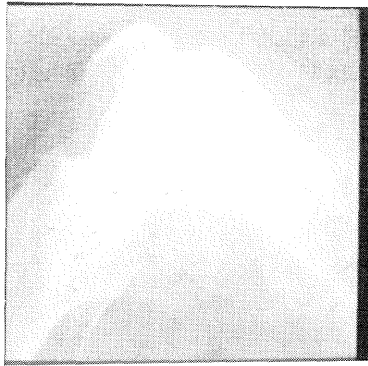


Figure 8. Spatial domain median filter 3\*3

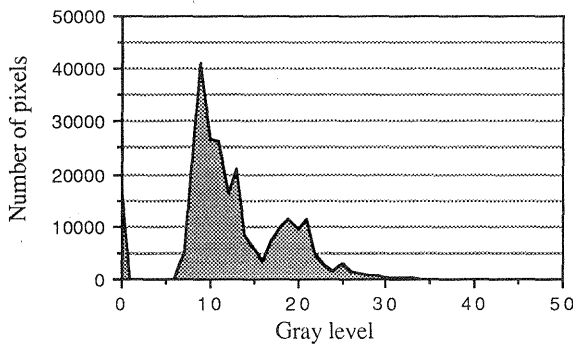


Figure 9. Histogram spatial domain 3\*3 median filter for image at 8.



Figure 10. Spatial domain mode filter 3\*3

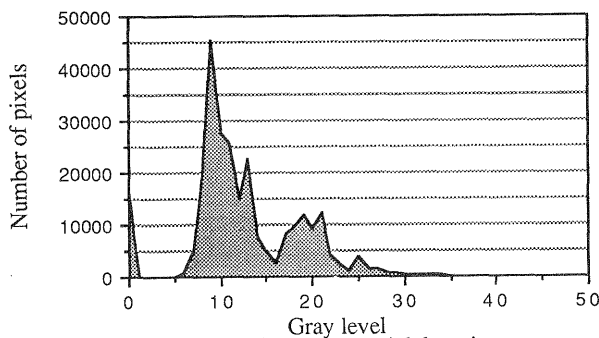


Figure 11. Histogram spatial domain 3\*3 mode filter for image at 10.

### Frequency domain

Prior to applying filters in the frequency domain, the power spectrum must be computed and displayed. Fast Fourier Transform (FFT) is used to transfer the image from spatial to frequency domain. The power spectrum is a graphical display of the horizontal and vertical frequency components of the image. Mathematically, this can be expressed as follows:

$$F(u, v) = \int_{-\infty}^{\infty} \int_{-\infty}^{\infty} f(x, y) \exp[-j2\pi(ux + vy)] dx dy \dots\dots\dots 2$$

$$f(x, y) = \int_{-\infty}^{\infty} \int_{-\infty}^{\infty} F(u, v) \exp[j2\pi(ux + vy)] du dv \dots\dots\dots 3$$

where:

$F(u, v)$  is the Fourier transformation of  $f(x, y)$ .

Equation 3 would transfer the image ( $f(x, y)$ ) from the spatial to frequency domain and 4 inverse it back. Equations 3 and 4 are referred to as Fourier transformation pairs. Fourier transformation of real function is generally contain real and imaginary terms.  $R(u, v)$  is the real and  $I(u, v)$  is the imaginary term respectively. The  $|F(u, v)|$  and  $|F(u, v)|^2$  are called Fourier spectrum, and power spectrum respectively.

$$|F(u, v)| = [R^2(u, v) + I^2(u, v)]^{1/2} \dots\dots\dots 4$$

$$P(u, v) = |F(u, v)|^2 = R^2(u, v) + I^2(u, v) \dots\dots\dots 5$$

The discrete form of equation 2 and 3 are:

$$F(u, v) = \frac{1}{N} \sum_{x=0}^{N-1} \sum_{y=0}^{N-1} f(x, y) \exp[-j2\pi(ux + vy) / N] \dots\dots 6$$

$$f(x, y) = \frac{1}{N} \sum_{u=0}^{N-1} \sum_{v=0}^{N-1} F(u, v) \exp[j2\pi(ux + vy) / N] \dots\dots\dots 7$$

where: all parameters are as previously defined.

Figure 12 shows the Log power spectrum of the image in figure 2. In general, high spatial frequencies correspond to areas of changing intensity on the image, such as areas containing noise, while low frequency components correspond to areas of less varying, or uniform, intensity. Ideal low-pass filter with cut-off frequency radii ranged from 0.25 to 2.75 inches was applied. Histograms and their corresponding images were collected at all cut-off frequencies (figure 13, 14, 15, and 16.)

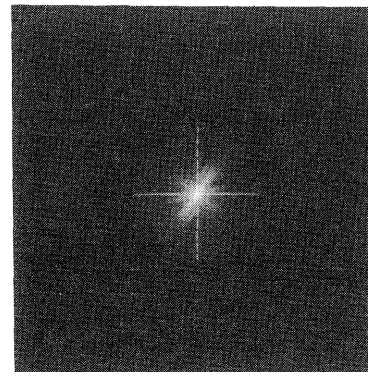


Figure 12. Log power spectrum of the original image

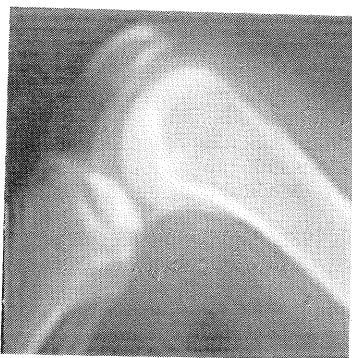


Figure 13. Frequency domain image at 0.25 inch radius.

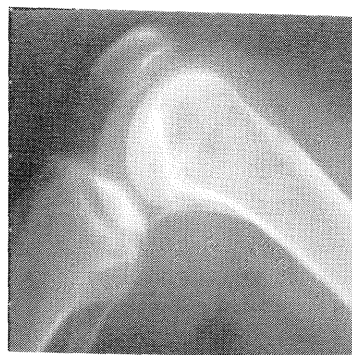


Figure 15. Frequency domain image at 2.75 inch radius.

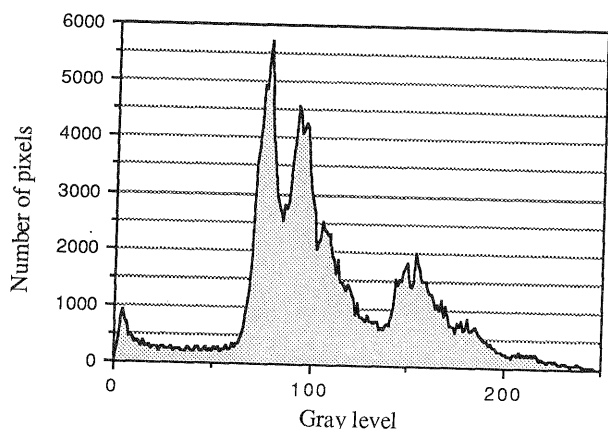


Figure 14. Frequency domain FFT at 0.25 inch radius.

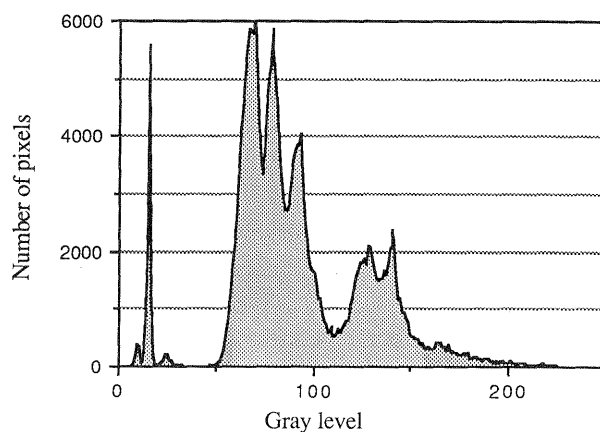


Figure 16. Frequency domain at 2.75 inch radius.

## RESULTS ANALYSIS

In the spatial domain, larger kernels size resulted in less noise and duller edges, regardless of filter type. The images generated from the median filter differed from the images resulting from a low-pass filter in that the edges were not as blurred, however, the differences were minimal. The mode filter generated images which contained more noise compared to either the low-pass or median filtered images.

Difference in the visual appearances of the obtained images can be seen, on the other hand, the histogram and statistic for all filters (table 1) show little or no variation. This is due to the original low contrast image.

In the frequency domain, a low-pass filter was applied to the power spectrum for various radii. In general, the larger the radius, the less it effect the noise. Larger radius is corresponded to smaller kernel size in the spatial domain. The physical appearances of the resultant images look different and once again the obtained histogram and statistic show little change (table 2). The ringing phenomenon can be seen only in frequency domain this can be easily explained by sorting to the convolution theorem (Gonzalez, 1987).

The decision as to which filter generates the "best" image based on physical appearance depends upon the application. For an X-ray image, the "best" image resulting from low-pass filtering would depend upon the use of the X-ray. Removing too much noise could result in losing vital details, while removing too little noise could result in vital details remaining obscured. This determination can be made to some extent by someone familiar with image processing, however, the final determination as to which is the "best" resulting X-ray image should be made by a qualified radiologist.

Table 1. Statistical data of Spatial Domain

filter	mean	std. dev	max (range)
original	12.51	6.08	40
LP 3x3	12.51	6.02	39
LP 5x5	12.50	6.01	38
LP 7x7	12.50	5.99	37
LP 9x9	12.50	5.97	38
MED 3x3	12.59	6.03	39
MED 5x5	12.59	6.02	38
MED 7x7	12.59	6.01	38
MED 9x9	12.58	5.99	37
MODE 3x3	12.60	6.04	40
MODE 5x5	12.61	6.04	40
MODE 7x7	12.60	6.04	40
MODE 9x9	12.60	6.03	40

Table 2. Statistical data of frequency Domain

FFT filter	mean	std. dev	max (range)
original	12.51	6.08	40
0.25 inch	106.80	43.35	254
0.5 inch	93.59	39.62	254
0.75 inch	89.16	38.11	253
1.0 inch	88.25	37.51	253
1.25 inch	89.22	37.07	255
1.5 inch	90.00	37.21	255
1.75 inch	91.26	36.82	255
2.75 inch	90.37	36.30	254

### Conclusion

As a result of applying low-pass filters to digital images using Imager software, the gray level histogram data is generated. The results of applying low-pass filters to an X-ray image to remove noise, show that the calculated statistics do not vary significantly from filter to filter within the spatial or the frequency domain. Also, within the spatial domain, the statistics do not vary significantly from kernel to kernel, and within the frequency domain, the statistics do not vary significantly from cut-off distance to another. Filtering in the frequency domain appears to maintain image integrity better than that of the spatial domain. In conclusion, the conventional noise removal techniques both in the spatial and frequency domains may not be an effective mean for noise removal in a rejected low contrast and noisy X-ray images. However, the final result depends mainly on the noise level in the image. Local adaptive box filter might be more effective in these case, since it tends to remove the noise locally rather than using the entire image.

### References

- Gonzalez, Rafael C., 1987. Digital Image Processing. Addison-Wesley, Reading, Massachusetts, pp 61-201
- Fahimi, H., Macovski, A., 1989 m. Reducing the effects of scattered photons in X-ray projection imaging. IEEE Transactions on Medical Imaging. 8 (1) : 56-63.
- Jain, Anil K., 1989. Fundamentals of Digital Image Processing. Prentice-Hall, New Jersey, pp. 431-471
- Jassam, Khalil, I. 1992, Image Processing of Conventional X-ray, International society of Photogrammetry and Remote Sensing.
- King, P. L., Browning, R., Pianetta P. and Lindau I., Keenlyside M. and Knapp G., 1989j. Image processing of multispectral X-ray photoelectron spectroscopy images. J. Vac. Sci. Technol. 7 (6): 3301-3304.
- Richards, John A. Remote Sensing and Digital Image Analysis: an introduction. New York: Springer-Verlag, 1986.
- Robb, R. A., Barillot, C., 1989s. Interactive display and analysis of 3-D medical images. IEEE Transactions on Medical Imaging. 8 (3) : 217-225.
- Sezan, M. I., Tekalp, A. M., Schaetzing, R., 1989j. Automatic anatomically selective image enhancement in digital chest radiography. IEEE Transactions on Medical Imaging. 8 (2) :154-163.
- Sherouse, G. W., Novins, K., Chaney, E. L., 1989. Computation of digitally reconstructed radiographs for use in radiotherapy treatment design. I. J. Radiation Oncology Biol Phys. 18 (3) : 651-658.
- TIGRIS Imager 1988. Intergraph Corporation, Huntsville, Alabama.
- Tahoces, P. G., Correa, J., Souto, M., Gonzalez, C., Gomez, L., Vidal, J. J., 1991s. Enhancement of chest and breast radiographs by automatic spatial filtering. IEEE Transactions on Medical Imaging. 10 (3): 330-335.